

Article

# Viscous Hydrodynamic Description of the Pseudorapidity Density and Energy Density Estimation for Pb+Pb and Xe+Xe Collisions at the LHC

Xiong-Tao Gong<sup>1,2</sup>, Ze-Fang Jiang<sup>1,3,4,\*</sup> , Duan She<sup>1,4</sup> and C. B. Yang<sup>1,4,\*</sup>

<sup>1</sup> College of Physical Science and Technology, Central China Normal University, Wuhan 430079, China; xggxt@mails.ccnu.edu.cn (X.-T.G.); sheduan@mails.ccnu.edu.cn (D.S.)

<sup>2</sup> Hubei Polytechnic Institute, Xiaogan 432000, China

<sup>3</sup> Department of Physics and Electronic-Information Engineering, Hubei Engineering University, Xiaogan 432000, China

<sup>4</sup> Key Laboratory of Quark and Lepton Physics (MOE) & Institute of Particle Physics, Wuhan 430079, China

\* Correspondence: jiangzf@mails.ccnu.edu.cn (Z.-F.J.); cbyang@mail.ccnu.edu.cn (C.-B.Y.)

Received: 23 March 2019; Accepted: 9 May 2019; Published: 10 May 2019



**Abstract:** Based on the analytical solution of accelerating relativistic viscous fluid hydrodynamics and Buda–Lund model, the pseudorapidity distributions of the most central Pb+Pb and Xe+Xe collisions are presented. Inspired by the CNC model, a modified energy density estimation formula is presented to investigate the dependence of the initial energy density estimation on the viscous effect. This new energy density estimation formula shows that the bulk energy is deposited to the neighboring fluid cells in the presence of the shear viscosity and bulk viscosity. In contrast to the well-known CNC energy density estimation formula, a 4.9% enhancement of the estimated energy density at the LHC kinematics is shown.

**Keywords:** viscous hydrodynamics; pseudorapidity distribution; energy density estimation

## 1. Introduction

Relativistic hydrodynamics is one of the most useful tools to investigate the space-time evolution and transport properties of the quark-gluon plasma (QGP) produced in high-energy heavy-ion collisions [1,2]. Besides numerical simulations, analytical solutions with simplified initial conditions are also useful in understanding the properties of this strongly coupled quantum chromodynamics (QCD) matter, such as the famous Hwa–Bjorken solution [3,4], Gubser solution [5], CGHK solution [6], CCHK solution [7], CNC solution [8,9], CKCJ solutions [10], and other interesting solutions [11–13]. In this paper, based on the well-known Buda–Lund model [14], an analytical solution of accelerating viscous relativistic hydrodynamics [15] is applied to investigate the final hadron pseudorapidity distribution and the energy density estimation. The charged particle pseudorapidity distributions ( $dN/d\eta_p$ ) for the most central  $\sqrt{s_{NN}} = 2.76$  TeV Pb+Pb collisions [16],  $\sqrt{s_{NN}} = 5.02$  TeV Pb+Pb collisions [17] and  $\sqrt{s_{NN}} = 5.44$  TeV Xe+Xe collisions [18] are presented. Based on this hydrodynamic model with longitudinal accelerating flow effect, the longitudinal acceleration parameters ( $\lambda$ ) are extracted from those experimental systems. Based on the CNC (Csörgő, Nagy, Csanád.) energy density estimation model [8,9] and its new results [10,19], a possible relationship between the energy density estimation and viscosity effect is also investigated.

This paper is organized as follows: in Section 2, we describe the hydrodynamic solutions and calculate the pseudorapidity densities. In Section 3, the energy density estimation and its viscosity dependence are investigated. A summary and discussion are given in Section 4.

## 2. Pseudorapidity Distribution from Hydrodynamics

The basic formulation of relativistic hydrodynamics can be found in the literature [20,21]. In this paper, we consider a system with net conservative charge ( $\mu_i = 0$ ). The flow velocity field is normalized to unity,  $u^\mu u_\mu = 1$  and the metric tensor is chosen as  $g_{\mu\nu} = \text{diag}(1, -1, -1, -1)$ .

Equations of hydrodynamics can be described by the following conservation laws

$$\partial_\mu(nu^\mu) = 0, \quad \partial_\mu T^{\mu\nu} = 0, \tag{1}$$

where the first one is the continuity equation of conserved charges and the second one is the energy-momentum conservation equations.  $n$  is a conserved charge and  $T^{\mu\nu}$  is the energy-momentum tensor. In the Landau frame, the energy-momentum tensor  $T^{\mu\nu}$  of the fluid, in the presence of viscosity, can be expressed as

$$T^{\mu\nu} = \varepsilon u^\mu u^\nu - P\Delta^{\mu\nu} + \Pi^{\mu\nu}. \tag{2}$$

In this expression,  $u^\mu$  is the velocity field,  $\varepsilon$  is the energy density,  $P$  is the pressure,  $\Pi^{\mu\nu} = \pi^{\mu\nu} - \Delta^{\mu\nu}\Pi$  is the viscous stress tensor with  $\Pi$  the bulk pressure and  $\pi^{\mu\nu}$  the stress tensor [20]. The projector  $\Delta^{\mu\nu} = g^{\mu\nu} - u^\mu u^\nu$  satisfies  $\Delta^{\mu\nu}u_\nu = 0$ . Please note that an Equation of State (EoS) is needed for the above conservation equations. For that,  $\varepsilon = \kappa P$  is frequently used with a constant  $\kappa$  value.

The simplest way to satisfy the second law of thermodynamics (entropy must always increase locally) is to impose the linear relationships between the thermodynamic forces and fluxes (in the Navier–Stokes limit [20,21]),

$$\Pi = -\zeta\theta, \quad \pi^{\mu\nu} = 2\eta\sigma^{\mu\nu}, \tag{3}$$

where the bulk viscosity  $\zeta$  and the shear viscosity  $\eta$  are two positive coefficients. Please note that throughout this work we denote the shear viscosity as  $\eta$ , the space-time rapidity as  $\eta_s$  and the particle pseudorapidity as  $\eta_p$ .

We solved the conservation equations  $\partial_\mu T^{\mu\nu} = 0$  in the Rindler coordinates and obtained a perturbative analytical solution of the relativistic viscous hydrodynamics with a longitudinally accelerating flow with constant shear viscosity to entropy density ratio and constant bulk viscosity to entropy density ratio (see detailed derivations in Ref. [15]). This analytical solution describes a finite size plasma produced in heavy-ion collision and is obtained from viscous hydrodynamics in the so-called Rindler coordinates by demanding rotational invariance around  $z$  and existing longitudinal pressure gradient along the beam direction.

The perturbative solution expression from the Ref. [15] is

$$u^\mu = (\cosh \lambda\eta_s, 0, 0, \sinh \lambda\eta_s), \tag{4}$$

$$T(\tau, \eta_s) = T_0 \left(\frac{\tau_0}{\tau}\right)^{\frac{1+\lambda^*}{\kappa}} \left[ \exp\left(-\frac{1}{2}\lambda^* \left(1 - \frac{1}{\kappa}\right) \eta_s^2\right) + \frac{R_0^{-1}}{\kappa - 1} \left(2\lambda^* + \exp\left[-\frac{1}{2}\lambda^* \left(1 - \frac{1}{\kappa}\right) \eta_s^2\right] - (2\lambda^* + 1) \left(\frac{\tau_0}{\tau}\right)^{\frac{\kappa-\lambda^*-1}{\kappa}}\right) \right], \tag{5}$$

here  $T_0$  is the temperature at the proper time  $\tau_0$ ,  $\tau$  is a coordinate at proper time,  $\eta_s$  is the space-time rapidity,  $\lambda = (1 + \lambda^*)$  controls the longitudinal acceleration,  $R_0$  is the Reynolds number and  $R_0^{-1} = \frac{\Pi_d}{T_0\tau_0}$ , and  $\Pi_d \equiv \left(\frac{\zeta}{s} + \frac{4\eta}{3s}\right)$  [20]. The profile of  $T(\tau, \eta_s)$  is a (1+1) dimensional scaling solution in (1+3) dimensions and it contains not only acceleration but also the viscosity dependent terms now, and the  $\eta_s$  dependence is of the Gaussian form. Please note that when  $\lambda^* = 0$  and  $R_0^{-1} = 0$ , one obtains the same solutions as the ideal hydrodynamics [4]. When  $\lambda^* = 0$  and  $R_0^{-1} \neq 0$ , one obtains the first order Bjorken solutions [20]. If  $\lambda^* \neq 0$  and  $R_0^{-1} = 0$ , one obtains a special solution which is consistent with case (c) in the CNC solutions in [8,9]. Furthermore, the temperature profile (5) implies that for

a non-vanishing acceleration  $\lambda^*$ , the cooling rate is larger compared to the ideal case. Meanwhile, a non-zero viscosity makes the cooling rate smaller than that of the ideal case.

Based on the Buda-Lund model and Cooper-Frye formula, the pseudorapidity distribution is calculated as follow [15]

$$\begin{aligned} \frac{dN}{d\eta_p} = & N_0 \int_{-\infty}^{+\infty} d\eta_s \int_0^{+\infty} dp_T \sqrt{1 - \frac{m^2}{m_T^2 \cosh^2 y}} m_T p_T \cosh((\lambda^* + 1)\eta_s - y) \\ & \times \exp \left[ -\frac{m_T}{T(\tau, \eta_s)} \cosh((\lambda^* + 1)\eta_s - y) \right] \left( \tau_f \cosh^{\frac{1-\lambda^*}{\lambda^*}}(\lambda^* \eta_s) + \frac{1 + \lambda^*}{T^3(\tau, \eta_s)} \right. \\ & \left. \times \left[ \frac{1}{3} \frac{\eta}{s} (p_T^2 - 2m_T^2 \sinh^2((\lambda^* + 1)\eta_s - y)) + \frac{1}{5} \frac{\zeta}{s} (p_T^2 + m_T^2 \sinh^2((\lambda^* + 1)\eta_s - y)) \right] \right), \end{aligned} \tag{6}$$

where  $N_0$  is the normalization parameter,  $m_T = \sqrt{p_T^2 + m^2}$  is the transverse mass,  $p_T$  is the transverse momentum,  $m$  is the particle mass,  $\eta_p$  is the pseudorapidity of the final hadron,  $y$  is the rapidity of the final particle, and we have the relationship:  $y = \frac{1}{2} \ln \frac{\sqrt{m^2 + p_T^2 \cosh^2 \eta_p + p_T \sinh \eta_p}}{\sqrt{m^2 + p_T^2 \cosh^2 \eta_p - p_T \sinh \eta_p}}$ .

### 3. Relationship between the Energy Density Estimation and Viscous Effect

As given in Bjorken’s paper [4], the phenomenological formula of the initial energy density estimation  $\epsilon_{Bj}$  is

$$\epsilon_{Bj} = \frac{1}{S_{\perp} \tau_0} \frac{d\langle E \rangle}{d\eta_p} = \frac{\langle E \rangle}{S_{\perp} \tau_0} \left. \frac{dN}{dy} \right|_{y=y_0}, \tag{7}$$

where  $S_{\perp}$  is area of the thin transverse slab at midrapidity. For the most central collisions of identical nuclei, the transverse area can be approximated as  $S_{\perp} = \pi R^2$ , with  $R$  being the nuclear radius,  $R = 1.18A^{1/3}$  fm.  $\langle E \rangle$  is the average energy of final particle,  $y_0$  is the middle rapidity  $\tau_0$  is the proper time at thermalization. This energy density was traditionally estimated by Bjorken as  $\tau_0 = 1\text{fm}/c$ , though the exact value of  $\tau_0$  is still a matter of debate. The volume element is  $dV = (R^2 \pi) \tau d\eta_s$ , where  $d\eta_s$  is the space-time rapidity element corresponding to the slab  $S_{\perp}$ . The energy content in this slab is  $dE = \langle m_t \rangle dN$ , with  $\langle m_t \rangle = \sqrt{\langle p_T \rangle^2 + m^2}$  from the  $\pi^{\pm}$ ,  $K^{\pm}$ ,  $p$  and  $\bar{p}$  average transverse momenta at midrapidity.

Based on the CNC energy density formula [8,9], for accelerationless, boost-invariant Hwa-Bjorken flow [3,4], the initial and final state space-time rapidities  $\eta_s$  are on the average equal to the hadron rapidity  $y$ . Thus, for a longitudinal accelerating flow, one must take:

$$\epsilon_{\text{corr}} = \epsilon_{Bj} \frac{dy}{d\eta_s^f} \frac{d\eta_s^f}{d\eta_s^i} = \epsilon_{Bj} (2\lambda - 1) \left( \frac{\tau_f}{\tau_0} \right)^{\lambda-1}, \tag{8}$$

where the upscript  $i$  and  $f$  indicate the initial state and final state,  $\lambda = \lambda^* + 1$ .

In addition, inspired by the recent CNC results [8,9,19], for the ideal flow, the formula of the initial energy density with the pressure evolution taken into account is:

$$\epsilon_{\text{corr}}^{\text{CNC}} = \epsilon_{Bj} (2\lambda - 1) \left( \frac{\tau_f}{\tau_0} \right)^{\lambda-1} \left( \frac{\tau_f}{\tau_0} \right)^{(\lambda-1)(1-\frac{1}{\kappa})}, \tag{9}$$

here  $\lambda$  is the longitudinal acceleration parameter,  $\kappa$  is a constant from the EoS,  $\tau_f$  is the freeze-out proper time.

For a viscous fluid, because the shear viscous tensor and bulk viscous pressure affect the pressure gradient (Equation (5)), the bulk energy is deposited to the neighboring fluid cells, which results in a system energy loss (or the so-called dissipative part in the midrapidity final yield). As one can see in

Equation (7), the initial energy density is calculated from the final state charged particle multiplicity from experiments at the midrapidity. Based on the final state spectrum (see Equation(6)), one finds that the viscosity effect reduces the particle multiplicity in the midrapidity ( $\left. \frac{dN}{dy} \right|_{y=y_0}$ ) because of the viscosity effect. In other words, if we take into account the viscosity effect for the energy density estimation from the midrapidity experimental data, the total energy at final state is lower than that in the initial state. Such dissipative effect can be calculated from Equation (5) and the EoS. Because of such difference, the energy density estimation based on the ideal fluid method would be lower than the viscous fluid method. Based on the above analysis, a possible energy density estimation, which considers the presence of accelerating flow effect and the viscous effect, can be presented as follows:

$$\epsilon_{\text{corr}}^{\text{viscous}} = \epsilon_{\text{Bj}}(2\lambda - 1) \left( \frac{\tau_f}{\tau_0} \right)^{\lambda-1} \left( \frac{\tau_f}{\tau_0} \right)^{(\lambda-1)(1-\frac{1}{\kappa})} \left[ 1 + \frac{(2\lambda - 1)R_0^{-1}}{\kappa - 1} \left( 1 - \left( \frac{\tau_0}{\tau_f} \right)^{\frac{\kappa-\lambda}{\kappa}} \right) \right]^{\kappa+1}, \quad (10)$$

where the square brackets term represents the enhancement from the viscosity (based on the thermodynamical evolution). From above expression, one can find: (a) if  $\lambda > 1$  and viscosity ratio  $\zeta/s = \eta/s = 0.0$ , it returns to the CNC energy density estimation Equation (9), (b) if  $\lambda \rightarrow 1$  and viscosity ratio  $\zeta/s = \eta/s = 0.0$  (or  $R_0^{-1} = 0.0$ ), it returns to the Bjorken energy density estimation Equation (7).

We present the numerical results for the pseudorapidity density and the energy density estimation in the Figure 1. In the left panel of Figure 1, the solid curves show the calculated pseudorapidity distribution. The normalization factor is determined from the most central multiplicity  $dN/d\eta_p(\eta_p = \eta_0)$  with the parameters  $\eta/s=0.16$  [22],  $\zeta/s=0.015$  [23]. The freeze-out temperature is  $T_f = 140$  MeV. For simplicity,  $\kappa \approx 7$  is assumed to be a constant in this study [24],  $m=220 \pm 20$  MeV is an approximate average mass of the final charged particle ( $\pi^\pm$ ,  $K^\pm$ ,  $p^\pm$ ) and it is calculated by a weighted average from the published experimental data [16]. The freeze-out proper time is chosen as  $\tau_f = 8$  fm. The rescatterings in the hadronic phase and the decays of hadronic resonance into stable hadrons are not included here. The acceptable integral region for each space-time rapidity in the model is  $-5.0 \leq \eta_s \leq 5.0$  (where the perturbative condition  $\lambda^* \eta_s \ll 1$  is satisfied). We then extracted the longitudinal acceleration parameters  $\lambda$  for 2.76 TeV Pb+Pb, 5.02 TeV Pb+Pb and 5.44 TeV Xe+Xe, the most central colliding systems without modifying any extra independent parameters. The values of  $\lambda$  for different colliding systems are listed in Table 1.

Having achieved a good description of the pseudorapidity distribution for Pb+Pb and Xe+Xe collisions, we move on to the calculation for the initial energy density. In Figure 1 right panel, the color bar shows the correction factor  $\epsilon_{\text{corr}}/\epsilon_{\text{Bj}}$  as a function of the ratio of freeze-out time and thermalization time ( $\tau_f/\tau_0$ ) for  $\lambda$  and viscosity ratio  $\zeta/s$  and  $\eta/s$ . The value of initial energy density is not calculated here, and we will present detailed discussion of this interesting problem in the near future as we did in Refs. [19,25]. Based on Equation (9), we found that the viscous effect results in an almost 4.9% enhancement for the energy density estimation when  $\tau_f/\tau_0 = 8$ . The correction factors  $\epsilon_{\text{corr}}/\epsilon_{\text{Bj}}$  are presented in Table 1 for different colliding systems.

**Table 1.** Parameters from hydrodynamic results in the text.

$\sqrt{s_{NN}}$	System	$\left. \frac{dn}{d\eta_p} \right _{\eta_p=\eta_{p0}}$	$\lambda$	$\epsilon_{\text{corr}}^{\text{CNC}}/\epsilon_{\text{Bj}}$	$\epsilon_{\text{corr}}^{\text{viscous}}/\epsilon_{\text{Bj}}$
2.76 TeV	Pb+Pb	$1615 \pm 39.0$	$1.035 \pm 0.003$	$1.225 \pm 0.022$	$1.285 \pm 0.022$
5.02 TeV	Pb+Pb	$1929 \pm 47.0$	$1.032 \pm 0.002$	$1.204 \pm 0.012$	$1.263 \pm 0.015$
5.44 TeV	Xe+Xe	$1167 \pm 26.0$	$1.030 \pm 0.003$	$1.190 \pm 0.021$	$1.248 \pm 0.022$

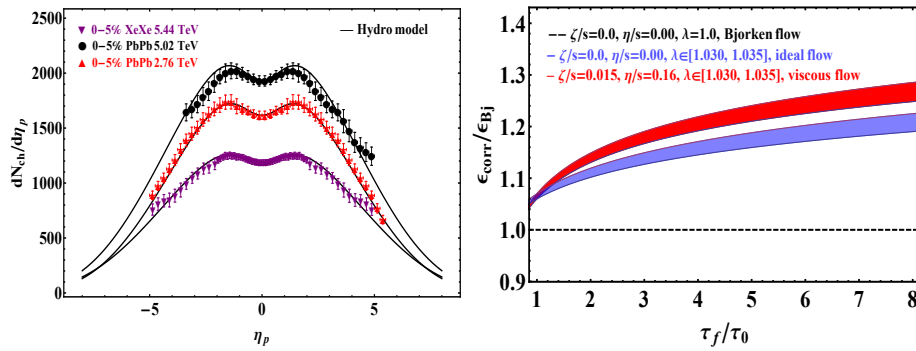


**Figure 1.** (Left): Pseudorapidity distribution from our model calculation (solid curves) compared to the LHC experimental data [16–18]. The black curves represent the pseudorapidity distribution for  $\sqrt{s_{NN}} = 2.76$  TeV Pb+Pb collisions,  $\sqrt{s_{NN}} = 5.02$  TeV Pb+Pb collisions and  $\sqrt{s_{NN}} = 5.44$  TeV Xe+Xe collisions. (Right): the correction factor  $\epsilon_{corr}/\epsilon_{Bj}$  as a function of the ratio of freeze-out time and thermalization time ( $\tau_f/\tau_0$ ) for different  $\lambda$  and shear viscosity ratio  $\eta/s$ , bulk viscosity ratio  $\zeta/s$ . The black dashed line is the result of Bjorken model, while the red band is the result that include the viscosity effect enhancement (Equation(10)), and the blue band is the result from Equation (9). The band width comes from the uncertainty of  $\lambda$  ( $-1.030 \leq \lambda \leq 1.035$ ). For the viscous fluid, the viscosity ratio is assumed to be constant [22,23] here and the statistical analysis of viscosity ratio is not discussed here.

#### 4. Conclusions and Discussion

In conclusion, the pseudorapidity densities and the viscosity dependence of the energy density estimation are presented in this paper based on an accelerating viscous hydro model and the experimental data for the Pb+Pb collisions and Xe+Xe collisions at the LHC energy region.

From the perturbative solution, one finds that the flow is generally decelerated due to the viscosity from the hydro solution, meanwhile, the longitudinal accelerating effect of the flow-element compensates for the decrease of pressure gradient. Those two opposite behaviors affect the thermodynamic evolution of the strong coupling QCD matter. Furthermore, from the final state expression and a good description of the experimental data at the LHC, one sees that the final state hadron spectrum is sensitive to the longitudinal flow effect. Simple modifications to the energy density estimation are proposed based on such two opposite behaviors, too. In contrast to the Bjorken model and CNC model, the viscosity effect results in a tiny enhancement for the energy density estimation. Detailed calculation of the energy density for different systems will be studied in next step.

In addition, it is also worth noting that we have made many simplifying assumptions in our hydrodynamic model, since our goal is only to show which longitudinal flow effect can be used to describe the pseudorapidity densities and to give a reasonable description for viscous effects dependence of the initial energy density estimation. For a more realistic study based on or beyond this study, the following physical effects are important and should be taken into account: the EoS, viscosity dependence (especially the bulk viscosity ratio taken from SU(3) pure-gluon lattice which is of large uncertainty about which there are recently suggestions that the full QGP value may actually be significantly larger than the lattice QCD results), freeze-out hypersurface calculation, resonance decay, and rescatterings in the hadronic phase and so on. Those important effects and conditions should be studied in our future research.

**Author Contributions:** Z.-F.J., X.-T.G. and D.S. performed the conceptualization, methodology, and validation of the energy density estimation viscosity dependence. Hydro model formal analysis is performed by Z.-F.J. and X.-T.G.; Z.-F.J. wrote the draft; C.B.Y., X.-T.G. and D.S. performed review and editing; All authors worked on finalization of the text of the manuscript.

**Funding:** This work was supported by the Sino-Hungarian bilateral cooperation program, under the Grand No. TeT 12CN-1-2012-0016, by the financial supported from NNSF of China under grant No.11435004.

**Acknowledgments:** We especially thank T. Csörgő, M. Csanád and the Organizers of the ZIMÁNYI SCHOOL/2018 for their kind hospitality and for an inspiring and useful meeting at Budapest, Hungary. We thank Xin-Nian Wang for a useful suggestion about xeon+xeon collisions. X.-T. Gong would like to thank the staff of College of Physical Science and Technology for kind hospitality during his stay at Institute of Particle Physics, Wuhan, China. Z.-F. Jiang would like to thank Lévai Péter and Gergely Gábor Barnafoldi for kind hospitality during his stay at Winger RCP, Budapest, Hungary.

**Conflicts of Interest:** The authors declare no conflict of interest.

## References

1. Bass, S.A.; Gyulassy, M.; Stöcker, H.; Greiner, W. Signatures of quark gluon plasma formation in high-energy heavy-ion collisions: A Critical review. *J. Phys. G Nucl. Part. Phys.* **1999**, *25*, R1–R57. [[CrossRef](#)]
2. Gyulassy, M.; McLerran, L. New forms of QCD matter discovered at RHIC. *Nucl. Phys. A* **2005**, *750*, 30–63. [[CrossRef](#)]
3. Hwa, R.C. Statistical Description of Hadron Constituents as a Basis for the Fluid Model of High-Energy Collisions. *Phys. Rev. D* **1974**, *10*, 2260. [[CrossRef](#)]
4. Bjorken, J.D. Highly Relativistic Nucleus-Nucleus Collisions: The Central Rapidity Region. *Phys. Rev. D* **1983**, *27*, 140. [[CrossRef](#)]
5. Gubser, S.S. Symmetry constraints on generalizations of Bjorken flow. *Phys. Rev. D* **2010**, *82*, 085027. [[CrossRef](#)]
6. Csörgő, T.; Grassi, F.; Hama, Y.; Kodama, T. Simple solutions of relativistic hydrodynamics for longitudinally expanding systems. *Acta Phys. Hung. A* **2003**, *21*, 53–62. [[CrossRef](#)]
7. Csörgő, T.; Csernai, L.P.; Hama, Y.; Kodama, T. Simple solutions of relativistic hydrodynamics for systems with ellipsoidal symmetry. *Acta Phys. Hung. A* **2004**, *21*, 73–84. [[CrossRef](#)]
8. Csörgő, T.; Nagy, M.I.; Csanád, M. A New family of simple solutions of perfect fluid hydrodynamics. *Phys. Lett. B* **2008**, *663*, 306. [[CrossRef](#)]
9. Nagy, M.I.; Csörgő, T.; Csanád, M. Detailed description of accelerating, simple solutions of relativistic perfect fluid hydrodynamics. *Phys. Rev. C* **2008**, *77*, 024908. [[CrossRef](#)]
10. Csörgő, T.; Kasza, G.; Csanád, M.; Jiang, Z.F. New exact solutions of relativistic hydrodynamics for longitudinally expanding fireballs. *Universe* **2018**, *4*, 69. [[CrossRef](#)]
11. Marrochio, H.; Noronha, J.; Denicol, G.S.; Luzum, M.; Jeon, S.; Gale, C. Solutions of Conformal Israel-Stewart Relativistic Viscous Fluid Dynamics. *Phys. Rev. C* **2015**, *91*, 051702. [[CrossRef](#)]
12. Hatta, Y.; Noronha, J.; Xiao, B.-W. Exact analytical solutions of second-order conformal hydrodynamics. *Phys. Rev. D* **2014**, *89*, 051702. [[CrossRef](#)]
13. Nopoush, M.; Ryblewski, R.; Strickland, M. Anisotropic hydrodynamics for conformal Gubser flow. *Phys. Rev. D* **2015**, *91*, 045007. [[CrossRef](#)]
14. Csörgő, T.; Lorstad, B. Bose-Einstein correlations for three-dimensionally expanding, cylindrically symmetric, finite systems. *Phys. Rev. C* **1996**, *54*, 1390. [[CrossRef](#)]
15. Jiang, Z.F.; Yang, C.B.; Ding, C.; Wu, X.-Y. Pseudo-rapidity distribution from a perturbative solution of viscous hydrodynamics for heavy ion collisions at RHIC and LHC. *Chin. Phys. C* **2018**, *42*, 123103. [[CrossRef](#)]
16. Adam, J.; et al. [ALICE Collaboration]. Centrality evolution of the charged-particle pseudorapidity density over a broad pseudorapidity range in Pb-Pb collisions at  $\sqrt{s_{NN}} = 2.76$  TeV. *Phys. Lett. B* **2016**, *754*, 373–385. [[CrossRef](#)]
17. Adam, J.; et al. [ALICE Collaboration]. Centrality dependence of the pseudorapidity density distribution for charged particles in Pb-Pb collisions at  $\sqrt{s_{NN}} = 5.02$  TeV. *Phys. Lett. B* **2016**, *722*, 567–577.
18. Acharya, S.; et al. [ALICE collaboration]. Centrality and pseudorapidity dependence of the charged-particle multiplicity density in Xe-Xe collisions at  $\sqrt{s_{NN}} = 5.44$  TeV. *arXiv* **2018**, arXiv:1805.04432.
19. Jiang, Z.-F.; Yang, C.B.; Csanád, M.; Csörgő, T. Accelerating hydrodynamic description of pseudorapidity density and the initial energy density in p+p, Cu + Cu, Au + Au, and Pb + Pb collisions at energies available at the BNL Relativistic Heavy Ion Collider and the CERN Large Hadron Collider. *Phys. Rev. C* **2018**, *97*, 064906.
20. Muronga, A. Causal theories of dissipative relativistic fluid dynamics for nuclear collisions. *Phys. Rev. C* **2004**, *69*, 034904. [[CrossRef](#)]

21. Romatschke, P. New Developments in Relativistic Viscous Hydrodynamics. *Int. J. Mod. Phys. E* **2010**, *19*, 1–53. [[CrossRef](#)]
22. Song, H.; Bass, S.A.; Heinz, U.; Hirano, T.; Shen, C. 200 A GeV Au+Au collisions serve a nearly perfect quark-gluon liquid. *Phys. Rev. Lett.* **2012**, *10*, 192301.
23. Meyer, H.B. Calculation of the bulk viscosity in SU(3) gluodynamics. *Phys. Rev. Lett.* **2008**, *100*, 162001. [[CrossRef](#)]
24. Pang, L.-G.; Petersen, H.; Wang, X.-N. Pseudorapidity distribution and decorrelation of anisotropic flow within CLVisc hydrodynamics. *Phys. Rev. C* **2018**, *97*, 064918. [[CrossRef](#)]
25. Jiang, Z.-F.; Csanád, M.; Kasza, G.; Yang, C.B.; Csörgő, T. Pseudorapidity and initial energy densities in p+p and heavy ion collisions at RHIC and LHC. *arXiv* **2018**, arXiv:1806.05750.



© 2019 by the authors. Licensee MDPI, Basel, Switzerland. This article is an open access article distributed under the terms and conditions of the Creative Commons Attribution (CC BY) license (<http://creativecommons.org/licenses/by/4.0/>).